NASA Technical Paper 1666

Experimental and Analytical Transonic Flutter Characteristics of a Geared-Elevator Configuration

Charles L. Ruhlin, Robert V. Doggett, Jr.,
and Richard A. Gregory

JUNE 1980

NASA

NASA Technical Paper 1666

Experimental and Analytical Transonic Flutter Characteristics of a Geared-Elevator Configuration

Charles L. Ruhlin and Robert V. Doggett, Jr.
Langley Research Center
Hampton, Virginia

Richard A. Gregory
Boeing Commercial Airplane Company
Seattle, Washington

National Aeronautics
and Space Administration

**Scientific and Technical
Information Office**

1980

SUMMARY

An experimental and analytical study has been made of the transonic flutter characteristics of an empennage model having an all-movable horizontal tail with a geared elevator. The model was an elastically and dynamically scaled version of the empennage and aft fuselage of a proposed supersonic transport airplane, and it was tested mounted from a low natural-frequency sting in the Langley Transonic Dynamics Tunnel. Two model configurations, namely, one with a geared elevator (gear ratio of 2.8 to 1.0) and one with an ungeared elevator (gear ratio of 1.0 to 1.0), were flutter tested. Symmetric flutter boundaries for the two configurations were experimentally determined over a Mach number range from 0.7 to 1.14. The geared-elevator configuration fluttered experimentally at dynamic pressures about 20 percent higher than did the ungeared-elevator configuration.

Symmetric flutter calculations were made only for the geared-elevator configuration. Two methods based on subsonic lifting-surface (kernel function) theory were used in the analyses. With both methods, the stabilizer and elevator were analyzed as a single, deforming surface. One of these methods also permitted the elevator to be analyzed as hinged from the stabilizer. All analyses predicted lower flutter dynamic pressures than experiment, with best agreement (within about 12 percent) obtained for the hinged-elevator method. The single, deforming surface methods, however, predicted flutter frequencies closer to the experimental values. Considering the model as mounted from a flexible rather than rigid sting in the analyses had only a slight effect on the flutter results but was significant in that a sting-related vibration mode was identified as a potentially flutter-critical mode.

INTRODUCTION

Take-off and transonic maneuvers of large supersonic transport airplanes require large trim changes which conventionally are controlled by deflecting the horizontal tail and/or elevators. For these airplanes, a tail design consisting of an all-movable horizontal tail with geared elevators has been proposed. The method of elevator gearing used in the present study is schematically shown in figure 1. It can be seen that gearing the elevator makes the tail aerodynamically more effective by allowing the elevator to rotate relative to the main tail surface as the all-movable-tail angle is changed, in effect, cambering the surface and producing higher lift for a given tail angle of attack as compared to a slab tail of the same size. Thus, elevator gearing provides a means of reducing tail size requirements which could save appreciable weight and cost for the airplane.

Although geared-elevator configurations are attractive from aerodynamic and performance points of view, there is concern about possible adverse effects on dynamic phenomena such as flutter. Unsteady aerodynamic theories are currently available to calculate the flutter characteristics of a lifting surface with control surfaces, but the application of such methods to geared-elevator

configurations has yet to be validated because no experimental data exist for comparison. The need for experimental flutter data becomes increasingly important at transonic speeds because flutter dynamic pressures are usually lowest in that regime and because existing unsteady aerodynamic theories are based on linear potential-flow considerations which exclude viscous-flow and shock-wave effects. In order to help provide a technology base for the flutter design of such configurations, an experimental and analytical flutter study of an all-movable horizontal tail with geared elevator was made, therefore, at transonic speeds.

The present study was limited primarily to hardware and mathematical structural models that had been developed previously for an existing flutter model. This model scaled dynamically and elastically the empennage and aft-fuselage section of a proposed supersonic transport airplane and had a geared-elevator configuration typical of those of current interest. The model was constructed by The Boeing Company but was not tested during the National Supersonic Transport Program and subsequently was made available by the Federal Aviation Administration to the National Aeronautics and Space Administration for the present tests. In the wind-tunnel tests, the model was attached to a long, low-frequency sting. The primary intent of the experiments was to determine the effect of elevator gearing on the tail symmetric flutter at transonic speeds. Wind-tunnel tests were made of two model configurations, one having a geared elevator (gear ratio of 2.8 to 1.0) and the other having an ungeared elevator (gear ratio of 1.0 to 1.0). The flutter tests were conducted in freon gas in the Langley Transonic Dynamics Tunnel at Mach numbers up to 1.14.

Flutter analyses were made for the geared-elevator configuration only. (The structural mathematical model for the ungeared-elevator configuration was never formulated during the earlier supersonic-transport development work.) This existing mathematical model did not include the effects of flexibility in the sting support; i.e., the model was considered as cantilevered from a rigid sting. Flutter calculations were made by using two analytical methods (refs. 1 and 2). Each method employed a modal-type analysis in which the unsteady aerodynamic forces were generated from subsonic, lifting-surface (kernel function) theory, and they differed mainly in numerical implementation and application. With both methods, flutter analyses were made with the stabilizer and elevator treated as a single, deforming surface. With the method of reference 1, flutter analyses were also made with the elevator treated as a surface hinged to the stabilizer with the aerodynamic singularities at the elevator hinge line accounted for.

The results of the aforementioned analyses and experiments were originally reported in reference 3. Subsequently, some errors were discovered in the computer-program implementation (ref. 4) for the hinged-surface portion of the method of reference 1. These errors have been corrected and some improvements have been made in this program (refs. 5 and 6). Also, since then, the structural mathematical model has been expanded to include the flexibility of the sting support. New flutter calculations were made by using this corrected, improved program and also by using the expanded mathematical model.

Presented herein and compared with the experimental results are these new analytical results. For completeness, the present paper includes from

reference 3 all the experimental results and those analytical results for which no corrections were necessary. Thus, the present report essentially corrects and replaces reference 3 and, in addition, shows the effect of the sting flexibility on the analytical flutter characteristics.

Use of trade names or names of manufacturers in this report does not constitute an official endorsement of such products or manufacturers, either expressed or implied, by the National Aeronautics and Space Administration.

MODEL AND MOUNT SYSTEM

General

Photographs of the model used in the present study are shown in figure 2, and some dimensional and structural details are presented in figures 3 and 4, respectively. The model represented a scaled version of the proposed supersonic-transport-airplane tail structure aft of the main rear wing spar and consisted of (see fig. 2) an aft fuselage, a vertical tail, and a horizontal tail. The horizontal tail and aft fuselage were geometrically, dynamically, and elastically scaled. Because symmetric flutter was of primary interest, the vertical tail was made overstiff to reduce the possibility of antisymmetric flutter, but its geometric and inertia scaling were maintained. The elevator hinge gap was small but not aerodynamically sealed.

Geometry

The horizontal tail (see fig. 3) consisted of the all-movable stabilizer and a full-span elevator. Each exposed horizontal-tail panel had an aspect ratio of 0.65, a taper ratio of 0.25, and a leading-edge sweepback angle of 54°. The elevator area was about 0.25 of the total-tail area with a hinge line located at a constant 0.74 chord (streamwise). Each exposed tail panel (excluding the carry-through structure) had a mass of about 3.4 kg (7.5 lbm) with a center of gravity as shown in figure 3. The stabilizer pitch axis was located at about the 40-percent chordwise station of the mean aerodynamic chord. Note that the tail-panel center of gravity is aft of the pitch axis. (See fig. 3.)

Early in the wind-tunnel flutter tests, the thin apex section of one tail-root leading edge (about 10 percent of the root chord) failed under the static aerodynamic loads. This section was rebuilt with a rounded leading-edge planform and, as a result, the rebuilt root chord was about 8 percent less than the original chord. The original planform is shown by the dashed lines in figure 3. The other tail panel was similarly altered for symmetry. All flutter data presented in this report are for this rounded apex planform.

Construction

The model was of monocoque construction. A partially exploded view showing some construction details of the horizontal tail is shown in

figure 4. Since both the left and right side panels of the horizontal tail were constructed similarly, only one panel is shown in figure 4 for simplicity. Load-carrying webs and most skin sections were made of a sandwich-type structure formed from a lightweight, plastic-foam core to which was bonded epoxy-laminated fiberglass sheets. The aft fuselage had thin bulkheads to provide an internal frame for the skin cover. The horizontal stabilizer and vertical tail were of similar construction and employed shear and rib webs covered by and bonded to the sandwich skins. For the thinner leading- and trailing-edge sections, a lightweight foam core was used between the fiberglass skins. The elevator had a fiberglass hinge beam, a foam center core, a trailing-edge closure section of balsa, and a skin covering of laminated fiberglass.

The horizontal stabilizer of the model was all-movable in pitch, and the stabilizer pitch angle was controlled remotely from the tunnel control room. The stabilizer pivot bracket (see fig. 4) was mounted to a fuselage bulkhead. Both the stabilizer and its pitch actuator arm were attached to the pivot bracket by a single pin in such a manner that each could rotate freely and independently about the common pinned joint. (For assembly, the right and left side panels of the stabilizer had been joined together. The pin connecting the stabilizer to the pivot bracket extended through the flange located at the front of the carry-through structural box of each panel.) The stabilizer was connected to the actuator arm by two steel leaf springs which bolted to the actuator arm and to the rear of the stabilizer carry-through structure. The actuator arm was also pinned to an articulated shaft extending from an electric motor and screw-type drive system located farther forward in the fuselage.

In order to change the stabilizer pitch angle, the electric motor was activated and, through the screw-type drive system, moved the articulated shaft forward or backward, thus forcing the actuator arm and the attached stabilizer to rotate in pitch about the pinned joint in the pivot bracket. The stiffnesses of the stabilizer pitch actuators of the airplane were simulated primarily by the two leaf springs on the model. (Normally, there were four pitch actuators on the airplane and they would have been simulated by four leaf springs on the model. For the present investigation, only two springs were used to insure low symmetric flutter dynamic pressures.)

The elevator was pinned to the stabilizer at five spanwise points along the elevator hinge axis. For the geared-elevator configuration (gear ratio of 2.8 to 1.0 or, more precisely, 2.77 to 1.0), the elevator spring and crank arrangement shown in figure 4 was used. It can be seen that when the stabilizer rotates in pitch, the elevator is forced to rotate about its hinge axis with the ratio (gear ratio) of the rotation angle of the elevator to that of the stabilizer fixed by the lengths of the elevator spring and crank. The left and right side elevators used the same crank but with individual elevator springs. For the ungeared elevator (gear ratio of 1.0 to 1.0), the elevator crank was removed and each elevator spring was replaced by a fiberglass beam which locked the elevator to the stabilizer and which provided nearly the same uncoupled elevator rotation frequency as the geared-elevator configuration.

Mount System

In the wind-tunnel tests, the aft fuselage of the model was cantilevered from a long, steel sting (fig. 2). The sting was very heavy and had a low natural frequency in an attempt to prevent sting-body coupling in the fundamental vibration modes. For example, the most forward sting section, which was about 3 m (10 ft) long, had a mass of over 500 kg (1102 lbm) as compared with the model total weight of 52 kg (115 lbm). An ogive nose section was attached to the forward end of the aft fuelage to provide streamlined flow. The sting base was attached through pins to a massive streamlined support strut which extended from floor to ceiling at the center of the wind tunnel. The sting could be traversed vertically or pitched in the tunnel as desired by jacking screws in the support strut.

Instrumentation

Model instrumentation included multiple strain-gage bridges on each stabilizer panel, strain gages and accelerometers on the fuselage, and angular-position transducers on the stabilizer, elevators, and sting. This instrumentation provided dynamic-response measurements of the bending and torsional deflections of the stabilizer, vertical translation, side translation, and twist of the fuselage, rotational (pitch) deflections of the stabilizer and elevators, as well as static measurements of the aerodynamic loading on the stabilizer and fuselage.

Experimental Vibration Characteristics

The measured node lines and frequencies associated with the symmetric natural-vibration modes of each model configuration are shown in figure 5, and the measured frequencies f and structural damping coefficients g for these modes are presented in table I. In the vibration surveys, the model was excited by a single, electromechanical shaker that was located near the rear of the fuselage tail cone and that provided a vertical sinusoidal force to the model. A lightweight, movable accelerometer was used to trace node-line patterns and determine phasing. The resonance frequencies and damping ratios were determined by the Kennedy-Pancu method using plots of the real and imaginary parts of the ratio of model response to input force.

The nodal patterns for the two model configurations were basically similar (see fig. 5), although the ungeared-elevator model had somewhat higher frequencies. Note that the fundamental bending-mode frequency of the sting (with the model attached) was about 1.9 Hz and that a coupled sting-empennage mode was measured at about 15 Hz for both model configurations. (See table I.)

Calculated Vibration Characteristics

The symmetric natural modes and frequencies of the geared-elevator configuration were calculated by using a finite-element structural analysis. Two

types of calculations were made. In the first type, the aft fuselage was considered to be cantilevered from the streamlined nose fairing and the sting was assumed to be rigid. This type will be referred to herein as the cantilevered case. In the second type, the aft fuselage was considered to be attached to the flexible wind-tunnel sting, and the effects of the sting mass and stiffness were accounted for in this analysis. This type will be referred to herein as the sting-mounted case.

Cantilevered case.- The stabilizer and elevator were modeled by using plate and beam elements; the actuators, linkages, and aft fuselage were modeled by using beam elements. Initially, the structure was idealized by using six substructures, namely, stabilizer, elevator, elevator linkage, inboard actuator, outboard actuator, and aft fuselage. The substructure matrices, which contained a total of 204 degrees of freedom, were merged and reduced to 125 degrees of freedom. The resulting equations of motion were then solved as an eigenvalue problem to determine natural frequencies and mode shapes.

The first six natural frequencies and associated node lines calculated for the cantilever case are presented in figure 6(b) and the frequencies are included in table I. The corresponding measured data from figure 5(a) are repeated in figure 6(a). A comparison of the calculated vibration characteristics with the experimental results shows that the analysis accurately predicted the modes that were composed primarily of horizontal-tail deformations for which the aft-fuselage bending effects of the sting flexibility were relatively unimportant. The first and third experimental modes were not predicted because the sting was an important factor in these modes.

Sting-mounted case.- The natural frequencies and mode shapes were calculated by using a component-mode-synthesis procedure. The two structural components were (1) the combined sting, sting-fuselage connection, and ogive nose with a rigid aft fuselage and empennage having the proper total mass and inertia characteristics, and (2) the elastic aft fuselage cantilevered from the nose fairing with elastic horizontal tail and rigid vertical tail. The second component was the same as for the cantilevered case. The modal characteristics of the first component were calculated by using a finite-element model composed primarily of beam elements, with a few plate elements used to represent the sting-fuselage connection structure. Pinned joints were used to approximate the attachment of the jacking screws in the tunnel support strut. The sting-mounted modal results were determined by combining the first 5 modes calculated for the first-component structure with the first 10 modes calculated for the second-component structure (cantilevered case modes) and taking the boundary conditions at the connection between the two components into account.

The first 10 calculated node lines and frequencies for the sting-mounted case are presented in figure 7. A comparison of the sting-mounted results with the cantilevered results (see table I and figs. 6 and 7) shows that including the sting effects introduced four additional modes in the frequency range from 0 to about 67 Hz. There is little difference between the frequencies and the node lines for the other six modes of the two cases. A comparison of the calculated modes with the measured modes (table I) shows that it was necessary to include the sting in the analysis in order to predict the two sting-related

modes at frequencies of 2 Hz and 15.4 Hz. Furthermore, the sting-mounted calculations also predicted two modes at frequencies of 38.8 Hz and 55.2 Hz that were not observed experimentally. There is good agreement in the other six modes, both between the two types of calculations and between the calculated and measured results.

PROCEDURE

Wind-Tunnel Flutter Tests

Test facility.- The model flutter tests were conducted in Freon[1] 12 in the Langley Transonic Dynamics Tunnel. This facility is a return-flow, variable-pressure, slotted-throat wind tunnel which has a 4.88-m-square (16-ft) test section with cropped corners. It is capable of operation at stagnation pressures from near vacuum to slightly above atmospheric and at Mach numbers from 0 to 1.2. Mach number and dynamic pressure can be varied independently. The tunnel is equipped with four quick-opening bypass valves which can be opened to reduce rapidly the dynamic pressure and Mach number in the test section when flutter occurs.

Test technique.- During the tests, the outputs of selected model transducers were continuously recorded and visually monitored on direct-readout recording oscillographs and magnetic tape. At operator-designated test conditions, certain model and tunnel test parameters were digitized and printed automatically. Visual records of the model behavior were provided by high-speed motion pictures. The static loads on the horizontal tail and fuselage were visually monitored, and adjustments to the stabilizer and/or sting pitch angle were made as required during the test to minimize these loads. At selected test conditions, a real-time analyzer was used to obtain a frequency spectrum of the model response to the tunnel turbulence. During the tests these spectra were helpful in observing and tracking the model response in the various vibration modes and the buildup in the critical mode response to a flutter condition.

The usual test procedure was to select a stagnation pressure in the tunnel and slowly increase Mach number (and dynamic pressure) until either flutter or the tunnel maximum Mach number was obtained. This procedure was repeated at consecutively higher stagnation pressures until a boundary of dynamic pressures at which flutter occurred was traced over the Mach number region of interest. To insure that a near-minimum flutter dynamic pressure was obtained for each model configuration tested, at least one no-flutter run was made below the flutter boundary. At flutter, the tunnel bypass valves were opened and the flutter quickly subsided. Model flutter was observed easily from the control room. Data from the recording oscillographs were used primarily to measure the flutter frequency and to aid in identifying which modes were involved in the flutter.

---

[1]Freon 12: Registered trademark of E. I. du Pont de Nemours & Co., Inc.

Flutter Analysis

General.- A summary of the flutter analyses made for the present study is presented in table II. Flutter calculations were made only for the geared-elevator configuration (gear ratio of 2.8 to 1.0). For this configuration, two different mathematical structural models were used. One structural model included the flexibility effects of the sting to which the model was mounted (sting-mounted case), whereas the other considered the model as cantilevered from a rigid sting (cantilevered case).

For each of these mathematical models, two methods were used to calculate the flutter characteristics. Both methods employed a modal-type analysis in which the unsteady aerodynamic forces were generated from subsonic lifting-surface (kernel-function) theory. In the calculations, the unsteady aerodynamic forces were generated only for the horizontal tail, but the generalized masses consisted of contributions from all the model vibrating components which, in addition to the horizontal tail, included the vertical tail, aft fuselage, and, in the sting-mounted case, the sting also.

Stabilizer with hinged elevator.- One calculation method used the kernel-function procedure described in references 1 and 5. This method allows the elevator to be treated as a surface hinged to the stabilizer and accounts for aerodynamic flow singularities at the elevator hinge line. (The hinge is aerodynamically sealed.) The computer-program implementation of this method is described in reference 6. For these calculations, the stabilizer was treated as the main lifting surface and the elevator was treated as a trailing-edge control surface. Model flutter characteristics were calculated at Mach numbers of 0.706 and 0.872 (which matched two experimental values).

Stabilizer elevator as single deforming surface.- The computer-program implementation of the procedure of reference 5 provides the option of treating a lifting surface without control surfaces. Flutter calculations were made by using this procedure with the stabilizer and elevator treated as a single, combined surface with a deforming trailing-edge region to approximate the deflecting elevator. The calculations were made for Mach numbers of 0.706, 0.872, and 0.982, matching all of the subsonic experimental points.

Because the computer implementation of reference 5 was relatively new, it was considered worthwhile to validate this program further by comparing the aforementioned results to those obtained with a proven, accepted method. The method selected for the validation is in routine use for flutter calculations at the Langley Research Center and is a refined kernel-function method (ref. 7) based on that described in reference 2. This method also treats the stabilizer as a single, deforming surface similarly to that described previously. By using this method, flutter calculations for the cantilevered mathematical model (cantilevered case) were made and reported originally in reference 3 and, for completeness, are also included herein. This method was also used in the present study to calculate the flutter characteristics for the sting-mounted mathematical model. (See table II.) The calculations were made for the same Mach numbers as before, namely, 0.706, 0.872, and 0.982.

Procedure details.- Because the flutter analyses were restricted to the symmetric case, the unsteady aerodynamic forces were generated only for the stabilizer and elevator surfaces on the right-hand half span of the horizontal tail. For all flutter calculations, the flow was assumed parallel to the model root chord, that is, essentially parallel to the aft-fuselage body surface line. For the aerodynamic model, the tail planform was altered slightly to make the tip chord parallel to the root chord. This was done by rotating the tip-section chord in yaw about its midpoint. Flutter calculations were made by using cantilevered and sting-mounted modes - the first 6 modes for the cantilevered calculations and the first 10 for the sting-mounted calculations. Where available, measured natural frequencies and structural damping ratios were used with corresponding calculated mode shapes and generalized masses. For modes for which frequencies were not measured (for example, the sixth sting-mounted mode with a frequency of 38.8 Hz), calculated frequencies were used. For modes for which damping ratios were not measured, the average damping coefficient g for all modes was used ($g = 0.0172$). Thirty-six downwash collocation points were used, with six points located along each chord at six spanwise stations. Surface-spline functions (ref. 8) were used to interpolate the calculated modal displacements from the values at the structural grid points to the displacements and slopes at the points required by the aerodynamic theory. For the method that treated the stabilizer and elevator as a single, deforming surface, a single spline function was used. For the hinged-elevator method, two separate spline functions were used, one for the stabilizer and one for the elevator. The flutter equations were solved by using an automated velocity-damping V-g solution method essentially the same as that described in references 7 and 9.

RESULTS AND DISCUSSION

Experimental Results

Symmetric flutter boundaries were determined experimentally for the geared-elevator configuration (gear ratio of 2.8 to 1.0) and ungeared-elevator configuration (gear ratio of 1.0 to 1.0) at Mach numbers from about 0.7 to 1.14. The experimental results are compiled in table III and plotted in figure 8 as the Mach number variation of the experimental dynamic pressure required for flutter of each configuration. Figure 8 also lists the measured frequencies at each experimental flutter point. The wind-tunnel tests were terminated when the ungeared-elevator configuration was destroyed during flutter at a Mach number of 0.88. From the data records, it was surmised that the left-hand structural connection between the stabilizer and elevator failed, allowing the elevator to oscillate freely, and the flutter oscillations rapidly increased until the fuselage failed and the model was destroyed.

The experimental results (fig. 8) show that elevator gearing increased the horizontal-tail flutter dynamic pressure q at transonic speeds, with the geared-elevator configuration having about a 20-percent higher flutter dynamic pressure q than the ungeared-elevator configuration. Thus, gearing the elevator made this tail configuration better from a flutter standpoint. Both model configurations had nearly flat flutter boundaries at Mach numbers from

0.9 to 1.14. The high flutter dynamic pressure q at $M = 0.7$ for the geared-elevator configuration may be caused by variations in mass-density ratio as well as in Mach number because symmetric flutter dynamic pressure q is normally a function of mass-density ratio, especially at the relatively low mass-density-ratio values of about 3 to 10 for the present configuration. (The mass-density ratio is the ratio of tail-panel mass to the mass of the fluid enclosing the model in a volume circumscribed by rotating the tail panel 360° in pitch about its midchord.)

The symmetric flutter mode for both model configurations was observed to be composed of aft-fuselage bending, stabilizer pitch and bending, and elevator rotation. Typical frequency spectra obtained by using a real-time analyzer are presented in figure 9. These spectra were measured during the tests of the geared-elevator configuration, and each spectrum shows the relative amplitude of the model response to the tunnel turbulence at different q levels, but all at $M = 0.7$. The response plotted was obtained from a strain-gage transducer located to measure fuselage vertical-bending deflections. In the spectrum for the lowest value of q (fig. 9), several vibration modes can be identified: namely, sting fundamental bending (1.9 Hz), fuselage fundamental vertical bending (7.8 Hz), and the sting-empennage mode at 15.5 Hz. As q increases, the fuselage bending mode gradually increases in frequency and amplitude and, although not apparent from these spectra, probably couples with a higher frequency mode to form the flutter mode. Because the sting-associated modes at 1.9 Hz and 15.5 Hz remain at about the same frequencies, it was concluded that they were not involved in the flutter mechanism.

Comparison of Analyses and Experiments

Comparisons of the calculated and experimental flutter results for the geared-elevator configuration are presented in figures 10 and 11. The comparison for the cantilevered case is shown in figure 10; the comparison for the sting-mounted case is shown in figure 11.

The flutter dynamic pressures predicted by analyses are lower than the experimental values. The calculated results for both the cantilevered case and the sting-mounted case show that the experimental flutter dynamic pressures are predicted more accurately by the hinged-elevator method, whereas the experimental flutter frequencies are predicted more accurately by the single, deforming surface method. Note that the flutter dynamic pressures predicted by the hinged-elevator method were all within about 12 percent of the experimental values.

Comparison of the analytical results in which the model was treated as a single, deforming surface (figs. 10 and 11) shows that the flutter dynamic pressures calculated by using the method routinely used at the Langley Research Center (ref. 2) were appreciably higher and closer to experiment than those calculated by the method of reference 1. The flutter frequencies predicted by these two methods were essentially the same and very close to the experimental values. These variations in the calculated flutter dynamic pressures must be attributed to differences in the numerical procedures used in implementing

the two theoretical methods because both methods were formulated from the same, basic, subsonic lifting-surface (kernel-function) theory.

A comparison of the calculated results in figure 10 (cantilevered case) with those in figure 11 (sting-mounted case) shows that including the effects of the sting flexibility reduced the flutter dynamic pressure by about 5 percent. Thus, including the sting flexibility in the analyses made the predicted flutter dynamic pressures even more conservative relative to experiment. A similar trend was found in the flutter-frequency calculations: namely, the flutter frequencies calculated by the two deforming surface methods also decreased when the sting effects were included. However, this trend was not observed in the hinged-elevator calculations since including the effects of the sting resulted in a decrease in frequency at a Mach number of 0.706 and an increase in frequency at a Mach number of 0.872.

For the sting-mounted case an additional flutter root was found in the range of interest for both the deforming surface and hinged-elevator cases. This root was of the "hump" type; that is, it crossed the stability boundary in the velocity-damping V-g diagram, indicated an unstable range of velocity, and with increasing velocity recrossed the stability boundary to the stable region. The slope of the crossing was relatively small compared to the nearly vertical crossing in the V-g diagram that was used to obtain the results in figures 10 and 11. This hump root was associated with the sting-empennage mode and had a flutter frequency of about 15.8 Hz. It appears that this hump root is the analytical counterpart of the response that was observed experimentally in this mode. (See fig. 9.) It is important to know before the flutter tests if any sting-related vibration modes will be flutter critical so that these modes may be either altered to prevent their flutter or, at least, identified so that they can be carefully monitored during the flutter tests. It is recommended, therefore, that future flutter studies of similar sting-mounted models include the flexibility of the sting in the flutter analyses and that these analyses be made prior to the flutter tests.

CONCLUSIONS

An experimental and analytical study has been made of the transonic flutter characteristics of an empennage flutter model having an all-movable horizontal tail with a geared elevator. Two model configurations were flutter tested: namely, one with a geared elevator (gear ratio of 2.8 to 1.0) and one with an ungeared elevator (gear ratio of 1.0 to 1.0). The model was cantilever-mounted on a sting in the Langley Transonic Dynamics Tunnel. Flutter characteristics were calculated only for the geared-elevator configuration by using two methods which were based on subsonic, lifting-surface (kernel-function) theory. The results indicate the following conclusions:

1. The geared-elevator configuration fluttered experimentally at about 20 percent higher dynamic pressures than the ungeared-elevator configuration. Thus, gearing the elevator made this tail configuration better from a flutter standpoint.

2. For both configurations, the experimental flutter dynamic pressure remained nearly constant as the Mach number was varied from about 0.9 to 1.14.

3. All flutter analyses predicted lower flutter dynamic pressures than experiment with best agreement (within about 12 percent) for the analytical method which treated the elevator as a hinged control surface.

4. Best analytical-to-experimental agreement of the flutter frequencies was obtained with the analytical methods which treated the stabilizer and elevator as a single, deforming surface.

5. Although the inclusion of sting flexibility in the analyses had only a small influence on the flutter dynamic pressure (predicting values about 5 percent lower than when the sting was considered as rigid), the analyses did identify as potentially flutter critical a sting-related mode that became very lowly damped during the flutter tests. It is recommended, therefore, that future flutter studies of similar sting-mounted models include the sting flexibility in the flutter analysis.

Langley Research Center
National Aeronautics and Space Administration
Hampton, VA 23665
April 15, 1980

REFERENCES

1. Rowe, W. S.; Redman, M. C.; Ehlers, F. E.; and Sebastian, J. D.: Prediction of Unsteady Aerodynamic Loadings Caused by Leading Edge and Trailing Edge Control Surface Motions in Subsonic Compressible Flow - Analysis and Results. NASA CR-2543, 1975.

2. Watkins, Charles E.; Woolston, Donald S.; and Cunningham, Herbert J.: A Systematic Kernel Function Procedure for Determining Aerodynamic Forces on Oscillating or Steady Finite Wings at Subsonic Speeds. NASA TR R-48, 1959.

3. Ruhlin, Charles L.; Doggett, Robert V., Jr.; and Gregory, Richard A.: Geared-Elevator Flutter Study. Proceedings AIAA/ASME/SAE 17th Structures, Structural Dynamics, and Materials Conference, May 1976, pp. 598-607. (Also available as NASA TM X-73902, 1976.)

4. Redman, M. C.; and Rowe, W. S.: Prediction of Unsteady Aerodynamic Loadings Caused by Leading Edge and Trailing Edge Control Surface Motions in Subsonic Compressible Flow - Computer Program Description. NASA CR-132634, 1975.

5. Rowe, W. S.; Sebastian, J. D.; and Petrarca, J. R.: Reduction of Computer Usage Costs in Predicting Unsteady Aerodynamic Loadings Caused by Control Surface Motions - Analysis and Results. NASA CR-3009, 1979.

6. Petrarca, J. R.; Harrison, B. A.; Redman, M. C.; and Rowe, W. S.: Reduction of Computer Usage Costs in Predicting Unsteady Aerodynamic Loadings Caused by Control Surface Motions. NASA CR-145354, 1979.

7. Desmarais, Robert N.; and Bennett, Robert M.: User's Guide for a Modular Flutter Analysis Software System (Fast Version 1.0). NASA TM-78720, 1978.

8. Harder, Robert L.; and Desmarais, Robert N.: Interpolation Using Surface Splines. J. Aircr., vol. 9, no. 2, Feb. 1972, pp. 189-191.

9. Desmarais, Robert N.; and Bennett, Robert M.: An Automated Procedure for Computing Flutter Eigenvalues. J. Aircr., vol. 11, no. 2, Feb. 1974, pp. 75-80.

TABLE I.- NATURAL VIBRATION MODAL FREQUENCIES AND DAMPING RATIOS OF MODEL CONFIGURATIONS

[The flutter analyses of the geared-elevator configuration employed measured frequency f and damping g values (rather than calculated frequencies) when available for the vibration modes used in the analysis]

Mode	Geared-elevator configuration (gear ratio of 2.8 to 1.0)				Ungeared-elevator configuration (gear ratio of 1.0 to 1.0)	
	Calculated		Measured		Measured	
	Cantilevered	Sting-mounted	Sting-mounted		Sting-mounted	
	f, Hz	f, Hz	f, Hz	g	f, Hz	g
Sting bending	----	2.0	1.9	(a)	1.9	(a)
Aft-fuselage bending	7.5	7.1	7.0	0.012	7.3	0.017
Sting-empennage	----	15.4	15.4	0.008	15.5	0.011
Stabilizer pitch	19.5	19.7	21.1	0.028	24.4	0.018
Elevator rotation	30.9	29.6	32.0	0.024	32.5	0.023
Sting-empennage	----	38.8	(a)	(a)	(a)	(a)
Coupled	45.4	45.4	46.5	0.012	(a)	(a)
Coupled	47.9	47.9	47.9	0.023	47.7	0.014
Sting-empennage	----	55.2	(a)	(a)	60.9	0.013
Coupled	66.3	66.5	66.9	0.014	69.8	0.013

[a]Not measured.

TABLE II.- SUMMARY OF FLUTTER ANALYSES OF GEARED-ELEVATOR CONFIGURATION

(GEAR RATIO OF 2.8 TO 1.0)

[Symmetric flutter analyses were made for the conditions and cases indicated by check (✓) marks]

Structural math model used	Mach number analyzed	Stabilizer with hinged elevator	Stabilizer and elevator as single deforming surface	
		Analysis method of refs. 1 and 5	Analysis method of refs. 1 and 5	Analysis method of refs. 2 and 7
Sting-mounted case: Model cantilevered from flexible sting 10 symmetric vibration modes	0.706	✓	✓	✓
	0.872	✓	✓	✓
	0.982	Not analyzed	✓	✓
Cantilevered case: Model cantilevered from rigid sting 6 symmetric vibration modes	0.706	✓	✓	✓
	0.872	✓	✓	✓
	0.982	Not analyzed	✓	✓

TABLE III.- EXPERIMENTAL FLUTTER RESULTS

Mach number	Dynamic pressure, kPa	Velocity, m/sec	Density, kg/m^3	Flutter frequency, Hz
Geared-elevator configuration (gear ratio of 2.8 to 1.0)				
0.706	14.63	110.6	2.3939	11.6
.872	12.49	136.0	1.3513	10.6
.982	12.29	152.5	1.0570	10.5
1.131	12.19	173.7	.8076	10.0
Ungeared-elevator configuration (gear ratio of 1.0 to 1.0)				
0.884	10.27	137.0	1.0941	9.6
1.006	10.29	154.9	.8581	9.5
1.140	10.22	173.9	.6757	9.4

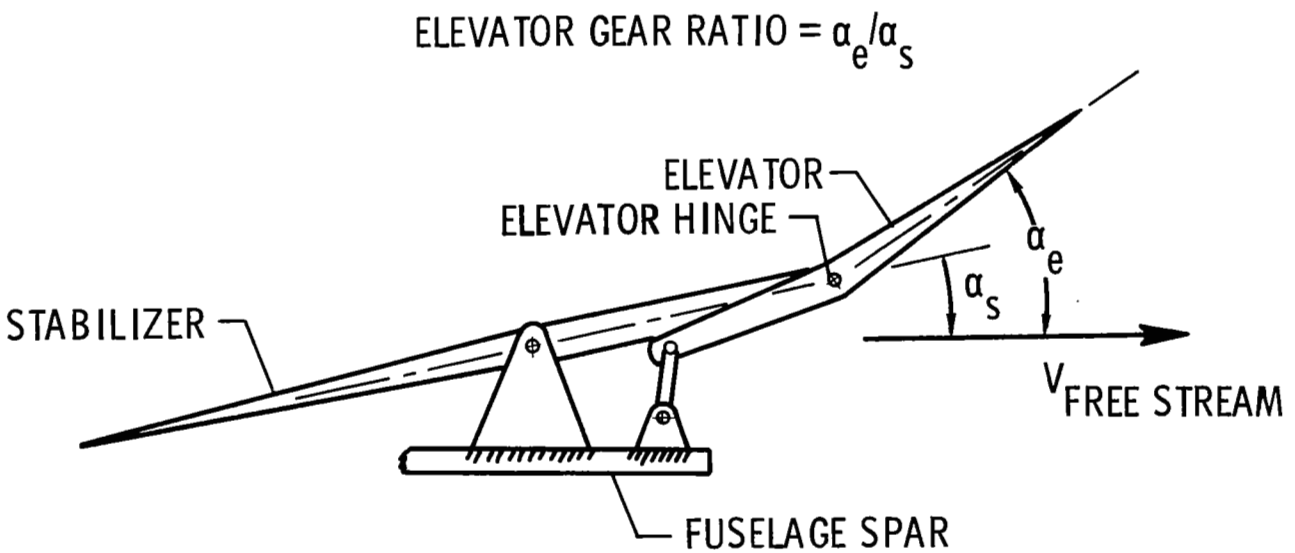

Figure 1.- Schematic drawing of elevator-gearing cranking arrangement.

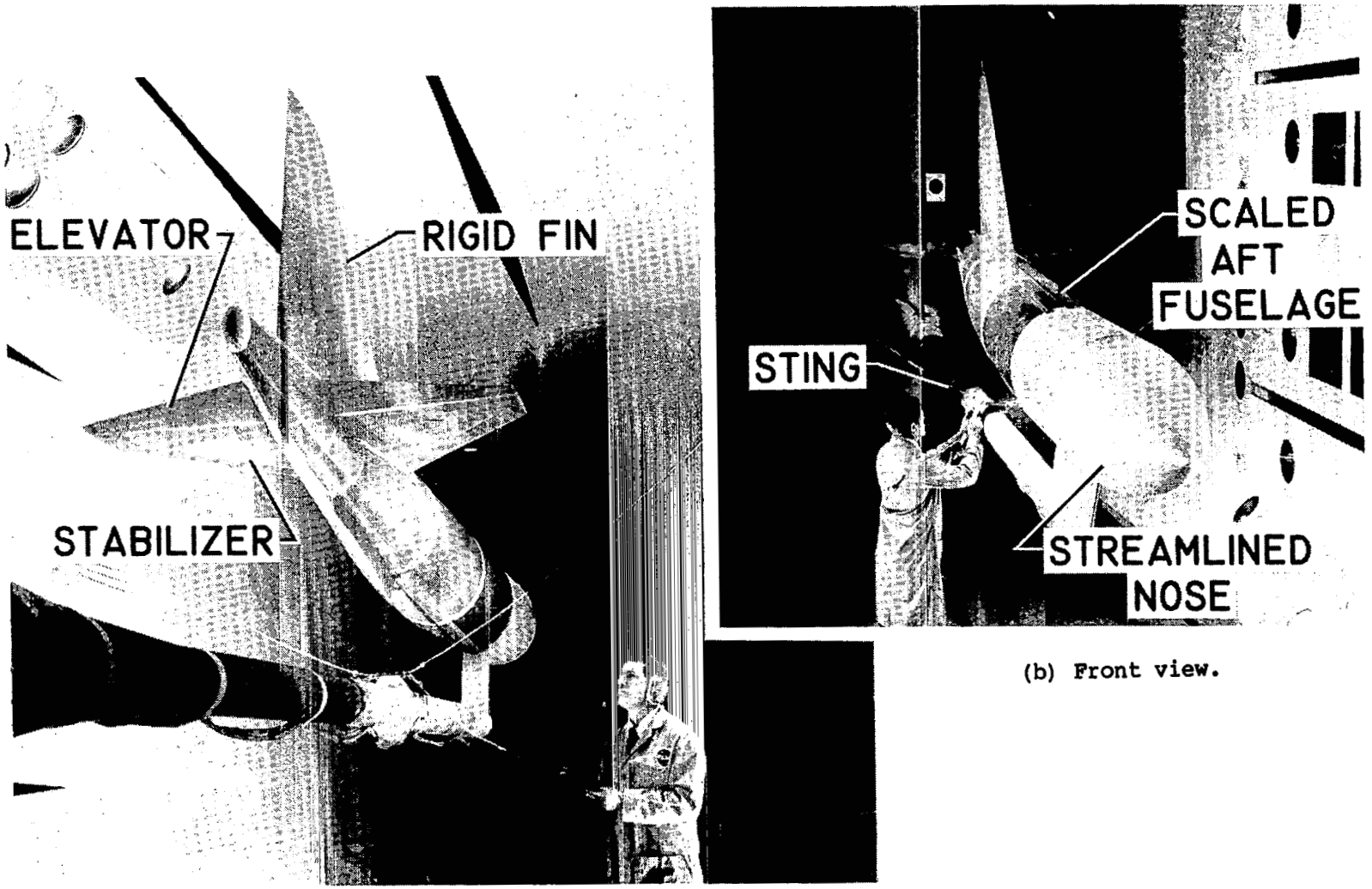

(a) Rear view.

(b) Front view.

L-80-128

Figure 2.- Photographs of model in wind tunnel.

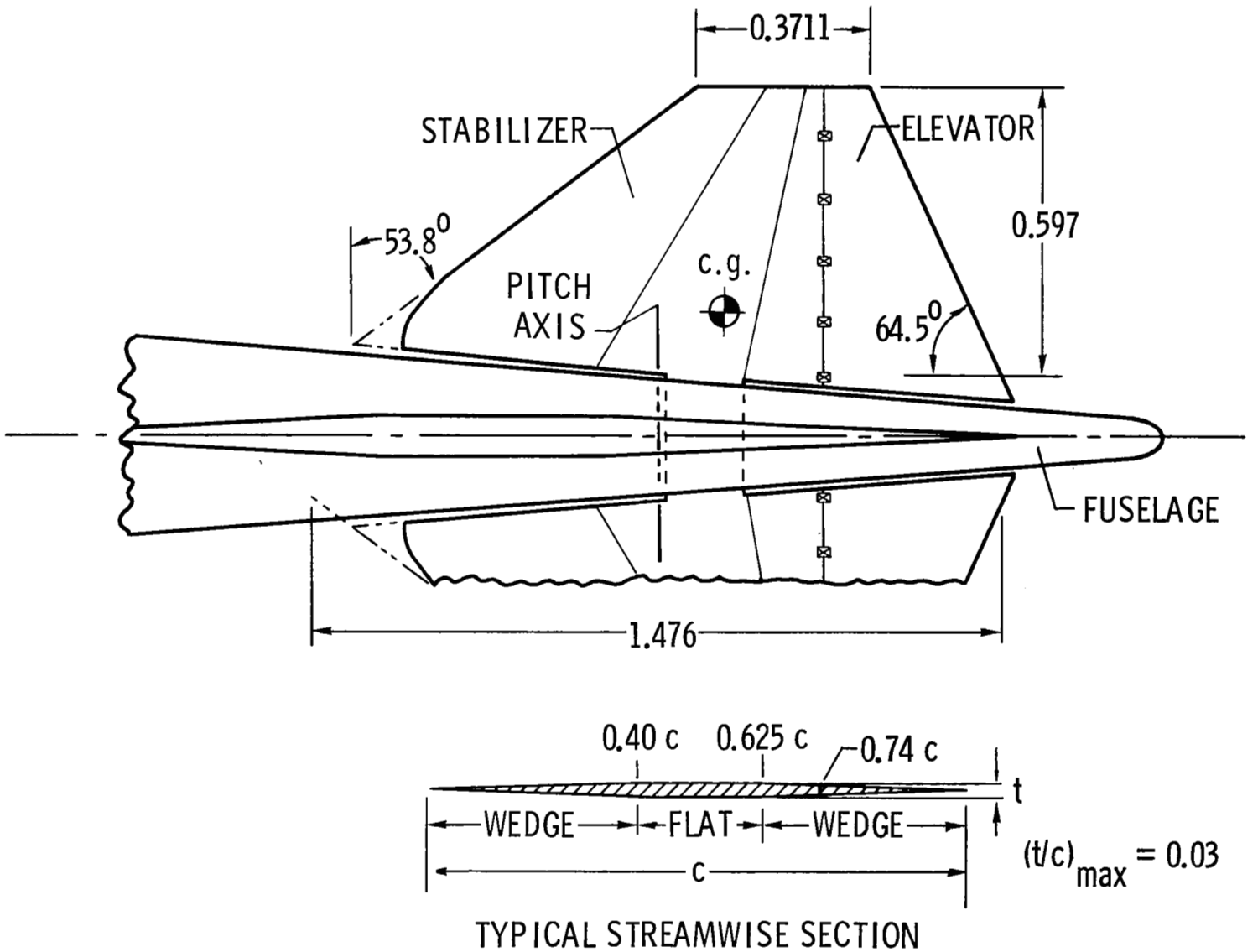

Figure 3.- Sketch of horizontal-tail model. Linear dimensions are in meters.

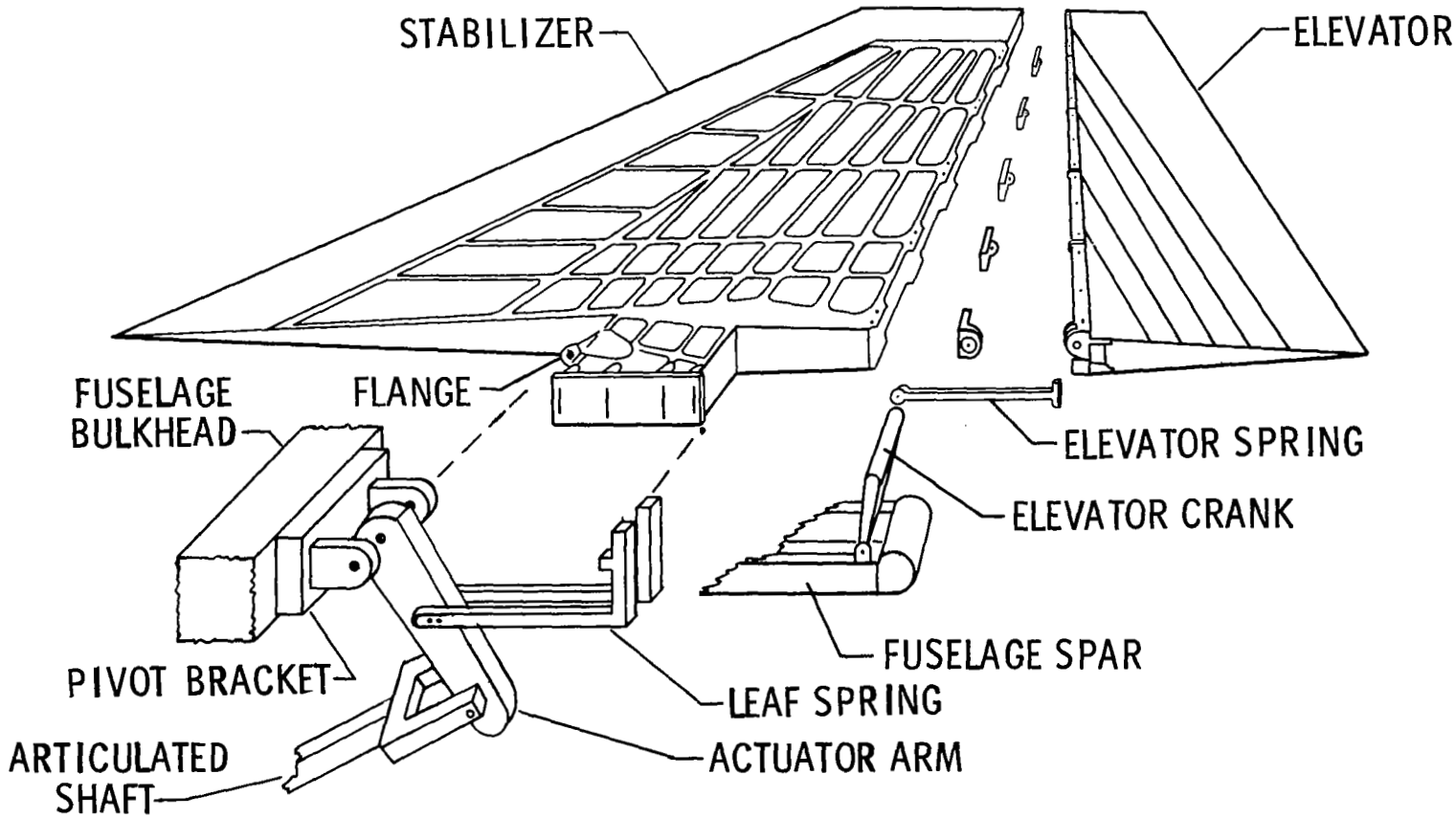

Figure 4.- Partially exploded view of horizontal tail.

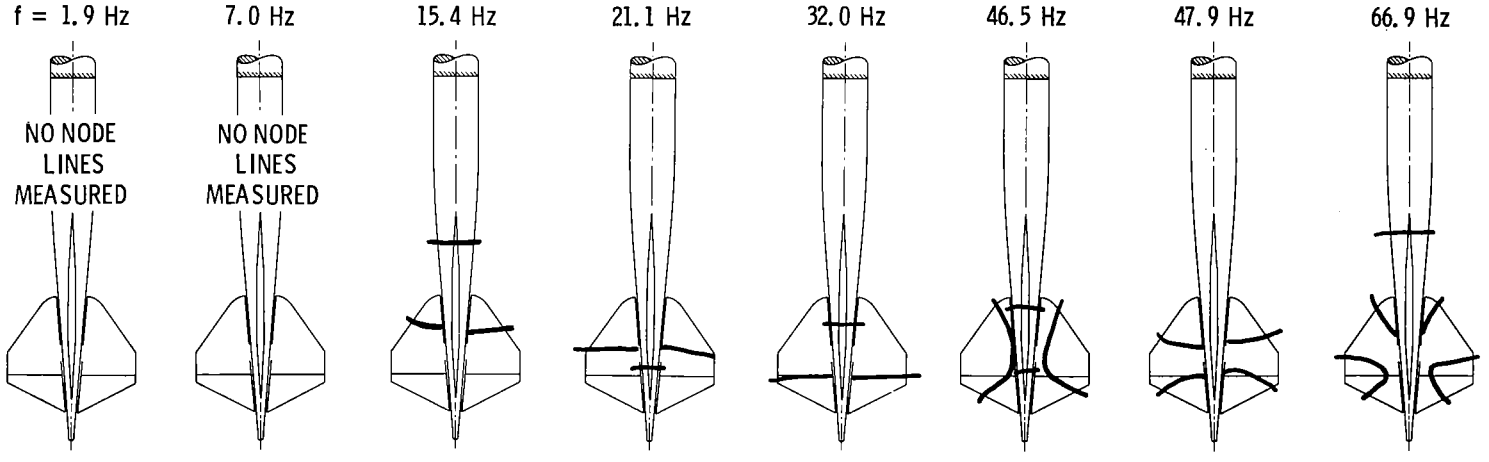

(a) Geared-elevator configuration (gear ratio of 2.8 to 1.0).

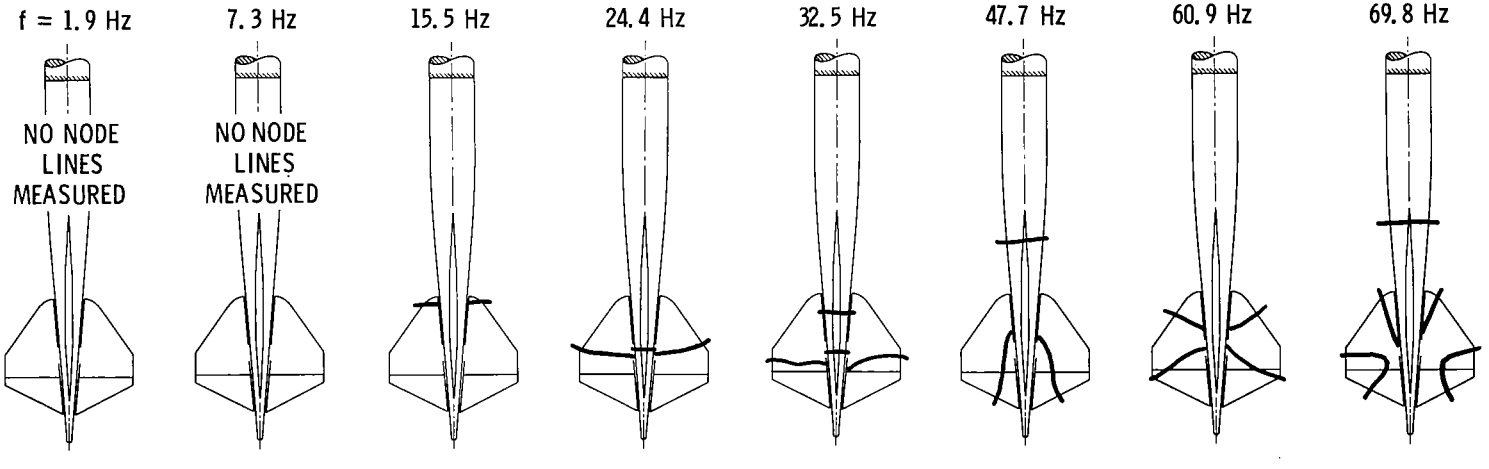

(b) Ungeared-elevator configuration (gear ratio of 1.0 to 1.0).

Figure 5.- Measured node lines and frequencies f of symmetric natural vibration modes of model configurations.

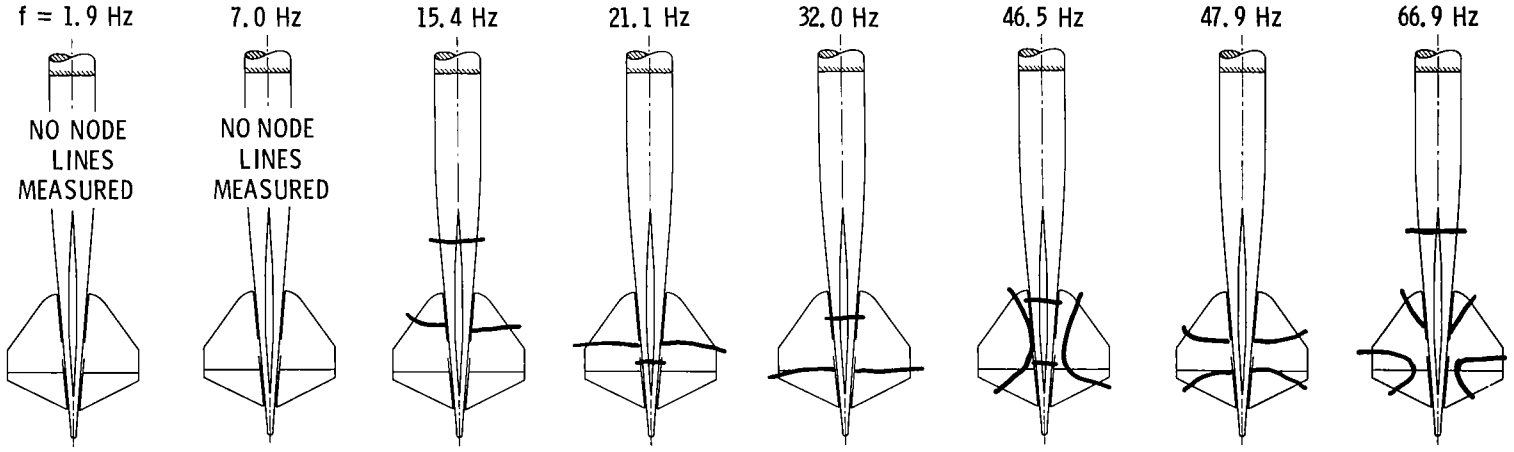

(a) Measured data.

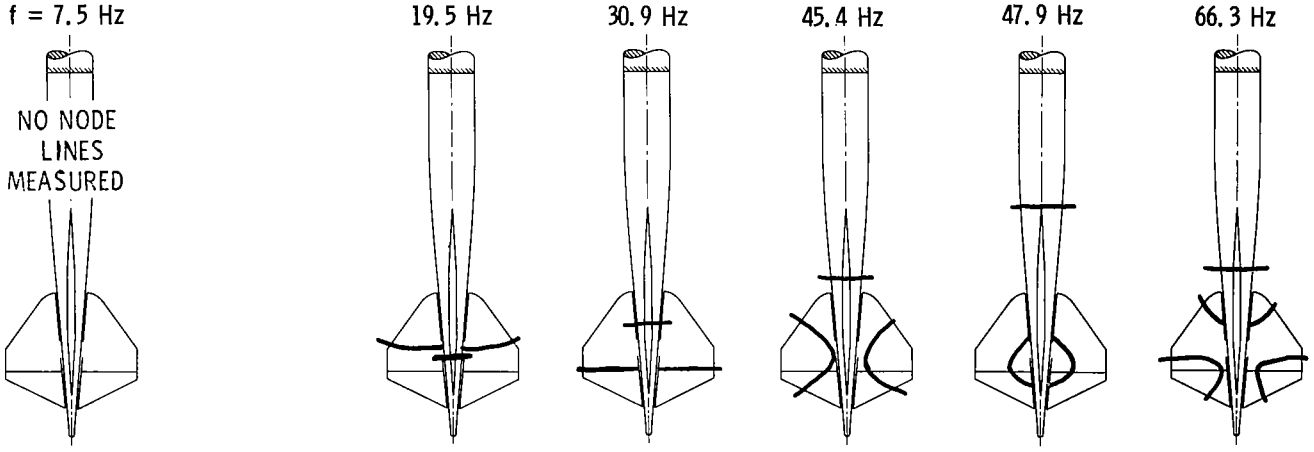

(b) Calculated data for cantilevered case.

Figure 6.- Measured and calculated node lines and frequencies f of symmetric natural vibration modes of geared-elevator configuration (gear ratio of 2.8 to 1.0). In the calculations the model is considered to be cantilevered from a rigid sting (cantilevered case).

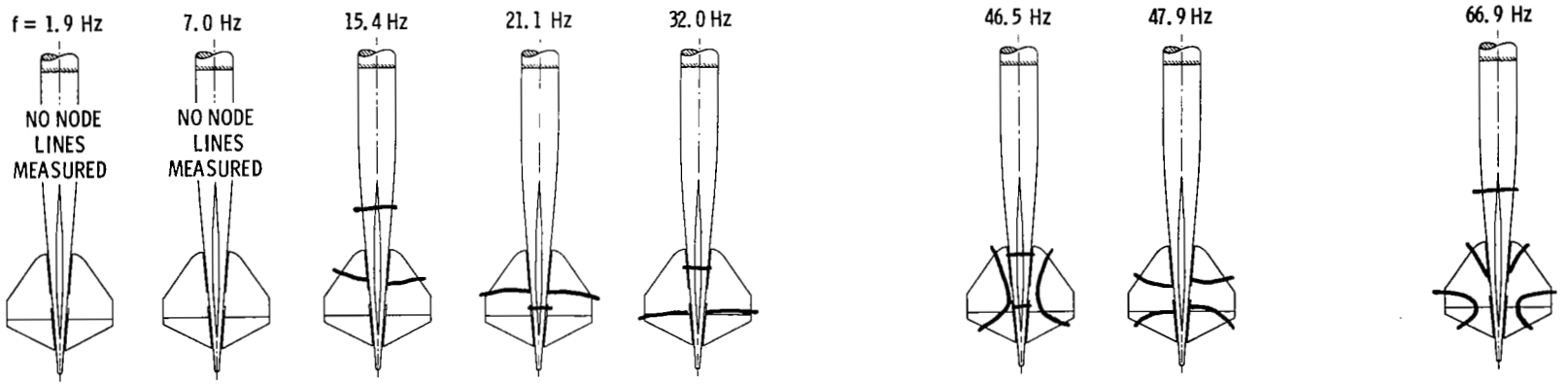

(a) Measured data.

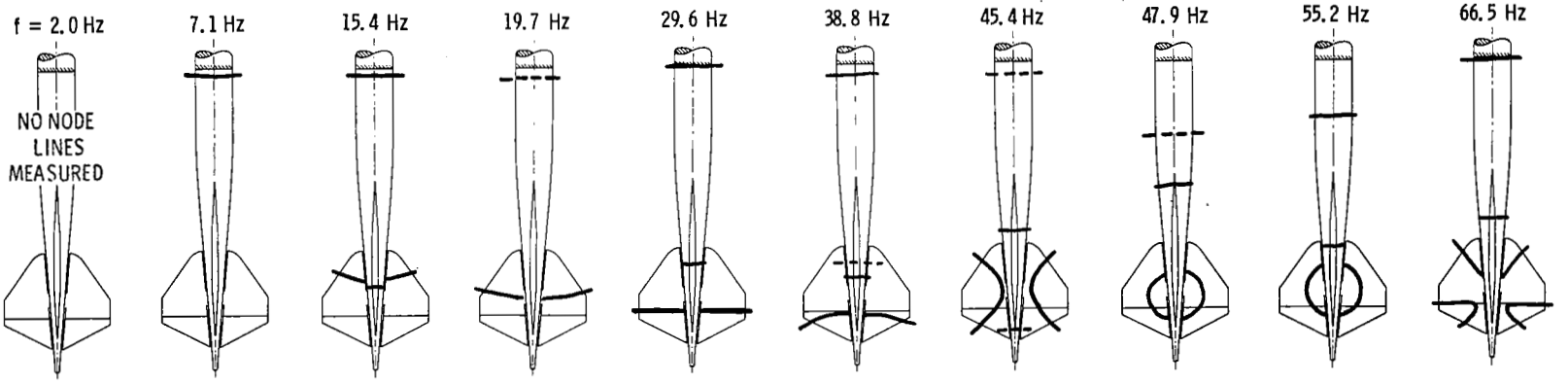

(b) Calculated data for sting-mounted case.

Figure 7.- Measured and calculated node lines and frequencies f of symmetric natural vibration modes of geared-elevator configuration (gear ratio of 2.8 to 1.0). In the calculations the model is considered to be cantilevered from a flexible sting (sting-mounted case). Dashed lines on calculated results designate node lines located on sting directly under model.

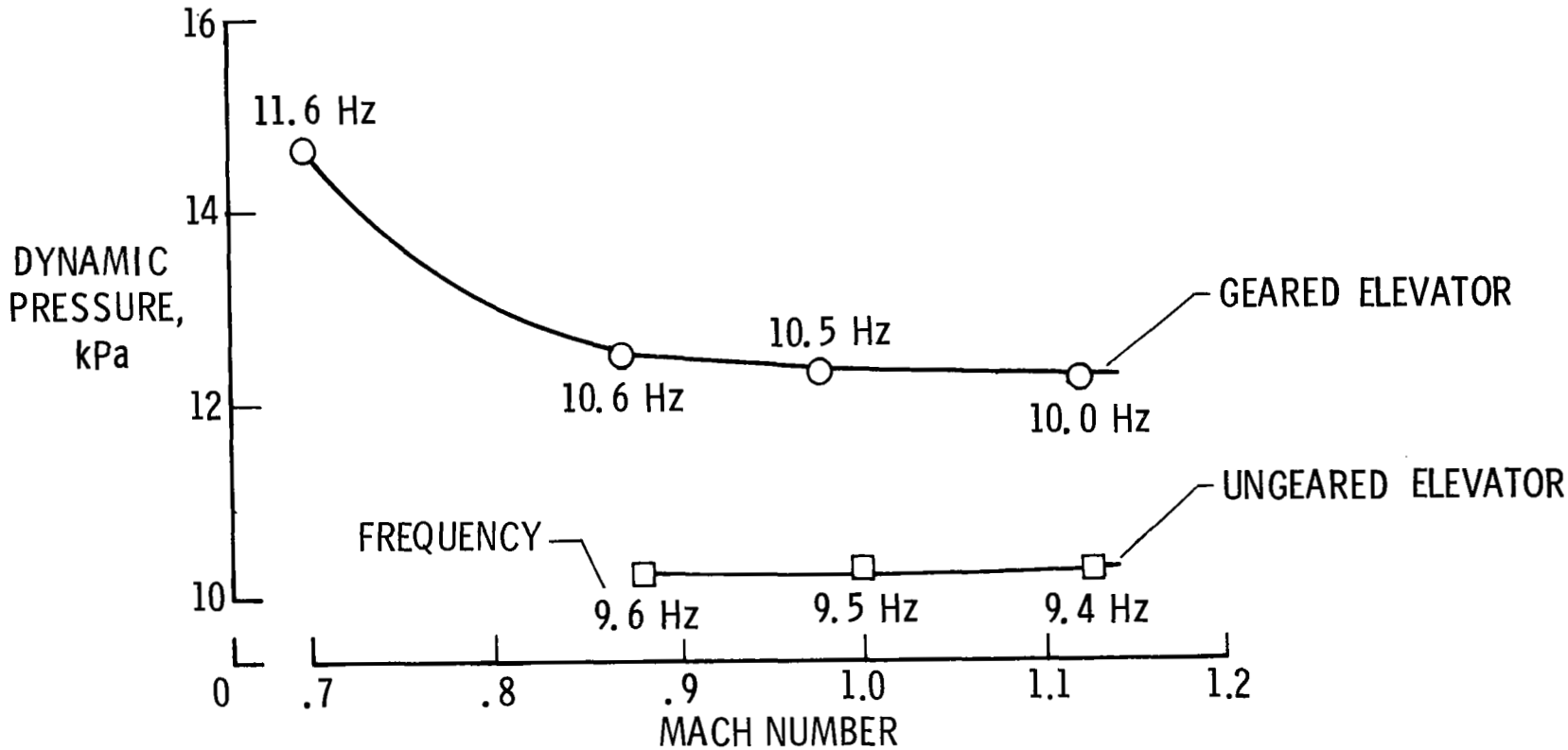

Figure 8.- Experimental flutter results for geared-elevator configuration (gear ratio of 2.8 to 1.0) and ungeared-elevator configuration (gear ratio of 1.0 to 1.0).

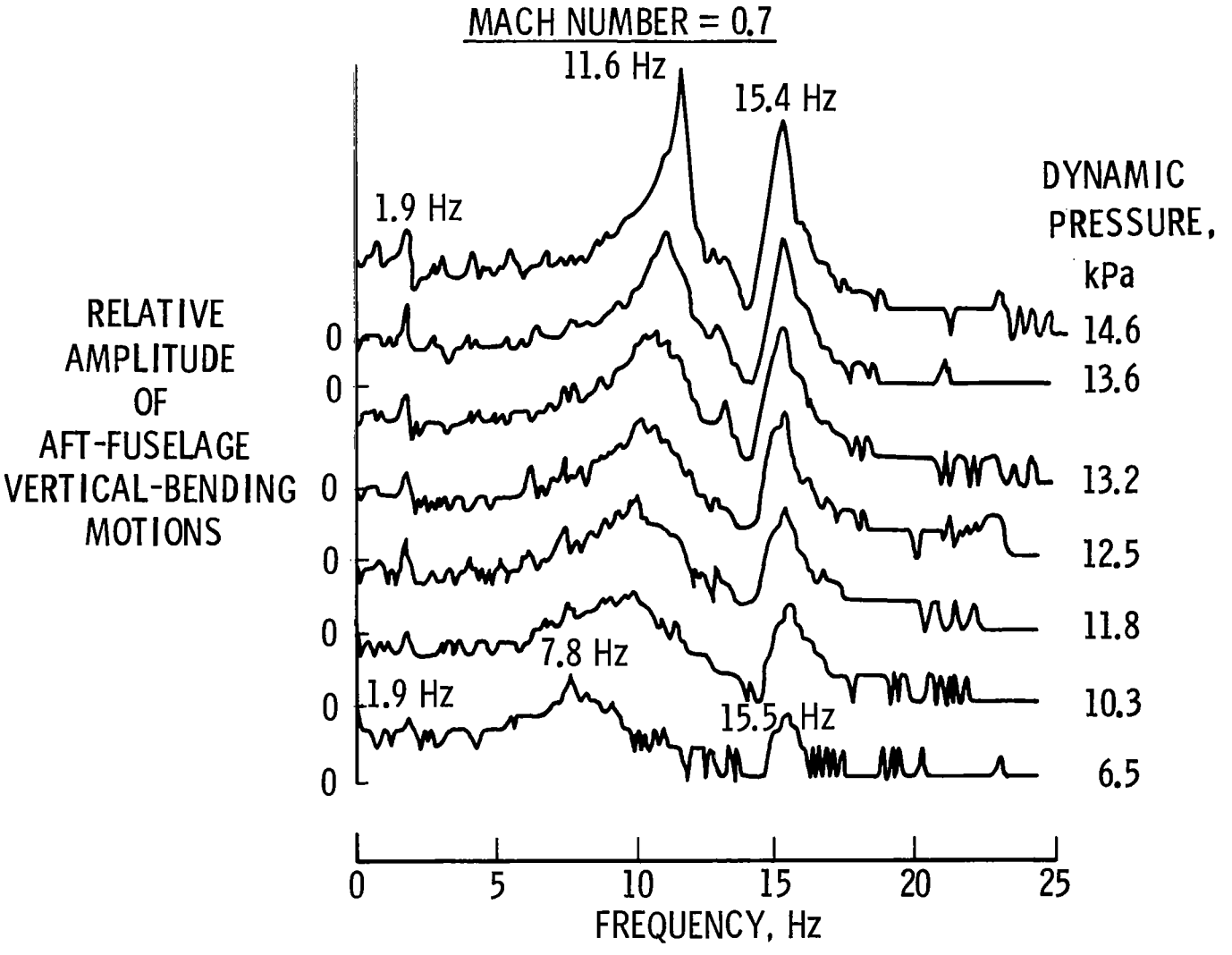

Figure 9.- Typical measured frequency spectra of model response to tunnel turbulence for the geared-elevator configuration (gear ratio of 2.8 to 1.0).

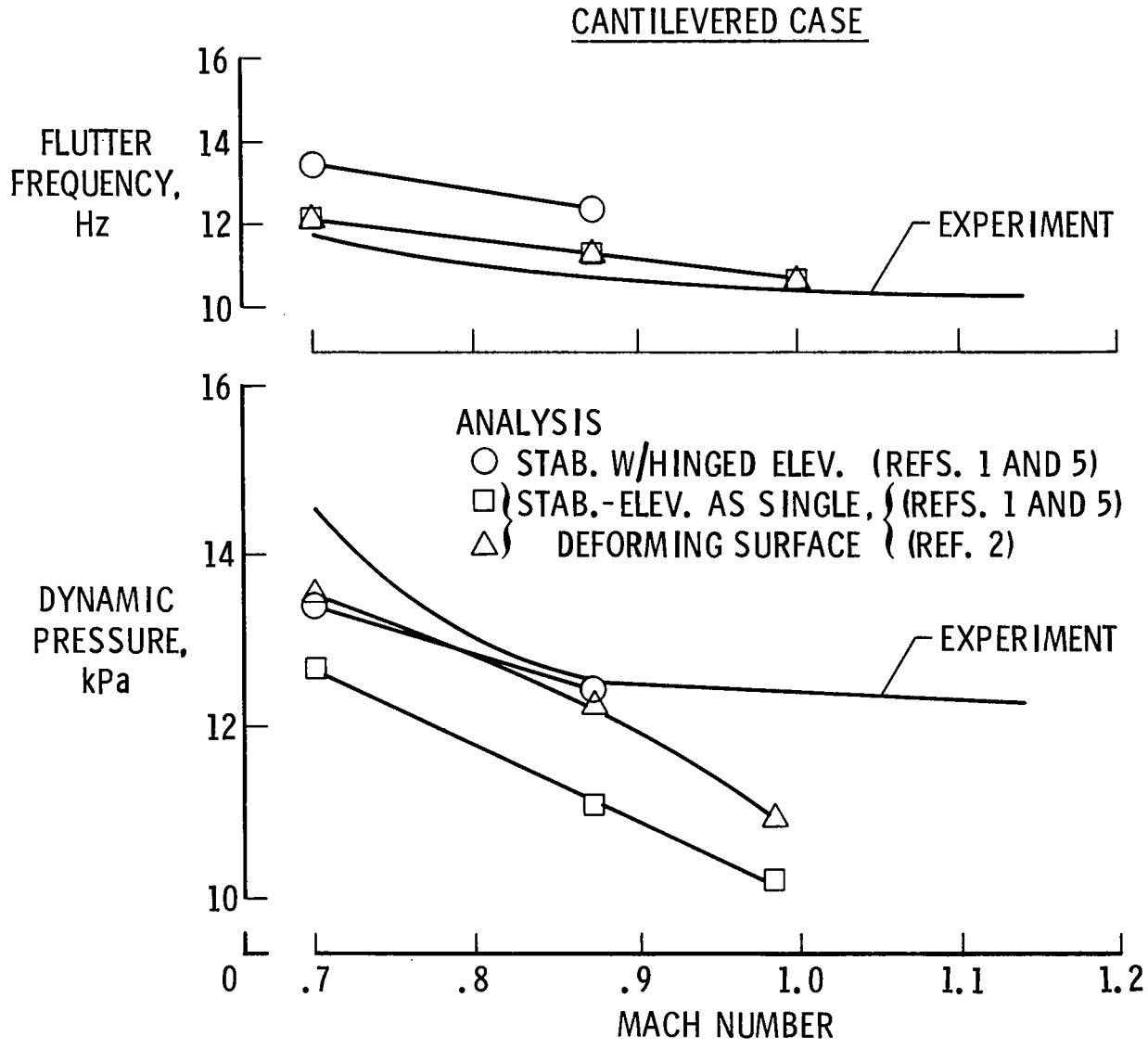

Figure 10.- Comparison of calculated and experimental flutter results for geared-elevator configuration (gear ratio of 2.8 to 1.0). In the analyses the model is considered as cantilevered from a rigid sting (cantilevered case).

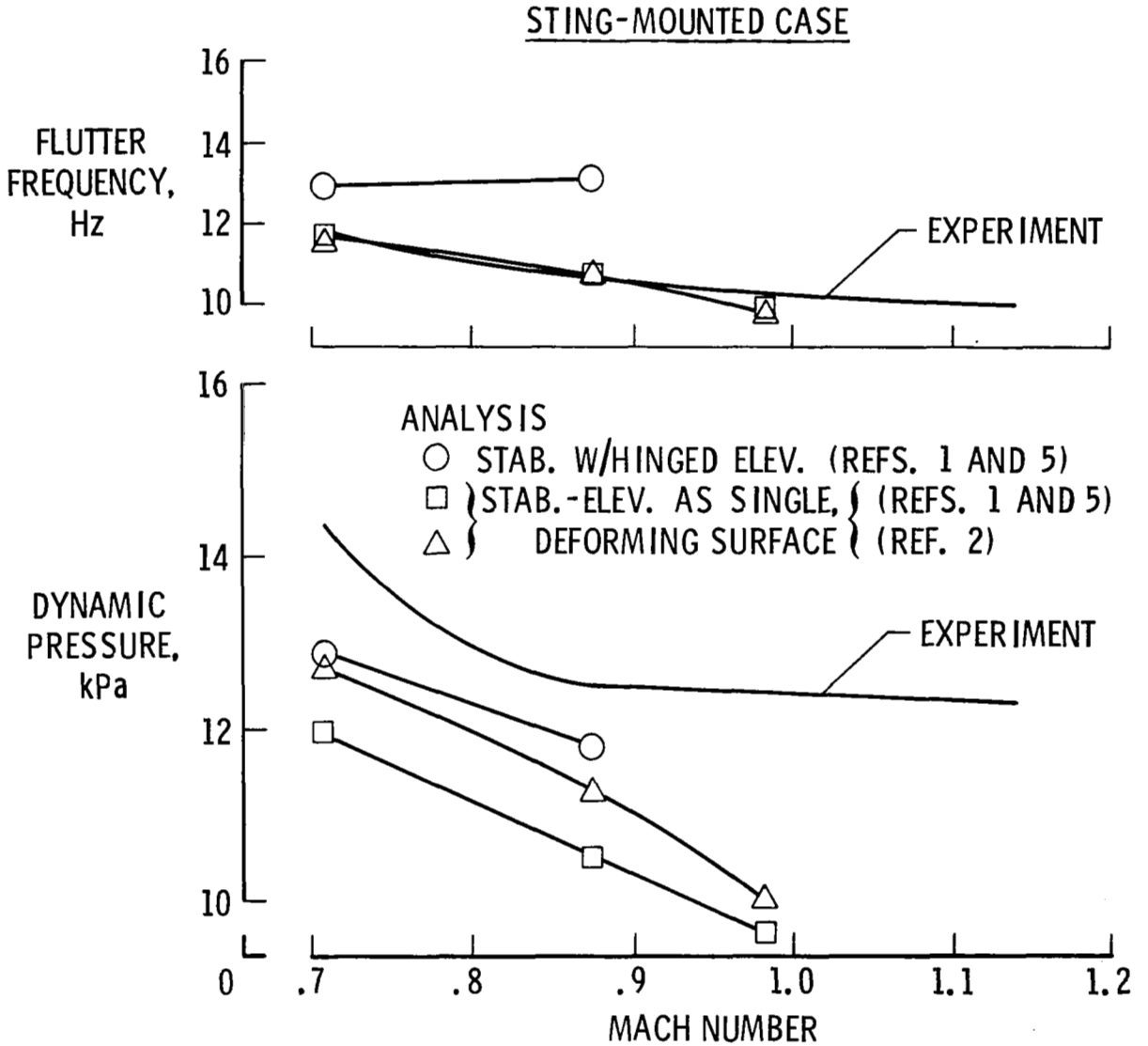

Figure 11.- Comparison of calculated and experimental flutter results for the geared-elevator configuration (gear ratio of 2.8 to 1.0). In the analyses the model is considered as cantilevered from a flexible sting (sting-mounted case).

1. Report No.	2. Government Accession No.	3. Recipient's Catalog No.
NASA TP-1666		

4. Title and Subtitle	5. Report Date
EXPERIMENTAL AND ANALYTICAL TRANSONIC FLUTTER CHARACTERISTICS OF A GEARED-ELEVATOR CONFIGURATION	June 1980
	6. Performing Organization Code

7. Author(s)	8. Performing Organization Report No.
Charles L. Ruhlin, Robert V. Doggett, Jr., and Richard A. Gregory	L-13544
	10. Work Unit No. 533-01-13-07

9. Performing Organization Name and Address	11. Contract or Grant No.
NASA Langley Research Center Hampton, VA 23665	
	13. Type of Report and Period Covered Technical Paper

12. Sponsoring Agency Name and Address	14. Sponsoring Agency Code
National Aeronautics and Space Administration Washington, DC 20546	

15. Supplementary Notes

Charles L. Ruhlin and Robert V. Doggett, Jr.: Langley Research Center.
Richard A. Gregory: Boeing Commercial Airplane Company, Seattle, Washington.

The present report corrects and replaces NASA TM X-73902 and a conference paper presented at the AIAA Conference on Structures, Structural Dynamics, and Materials in May 1976.

16. Abstract

The flutter model represented the aft fuselage and empennage of a proposed supersonic transport airplane and had an all-movable horizontal tail with a geared elevator. It was tested mounted from a sting in the Langley Transonic Dynamics Tunnel. Symmetric fluttter boundaries were determined experimentally at Mach numbers from 0.7 to 1.14 for a geared-elevator configuration (gear ratio of 2.8 to 1.0) and an ungeared-elevator configuration (gear ratio of 1.0 to 1.0). Gearing the elevator increased the experimental flutter dynamic pressures about 20 percent. Flutter calculations were made for the geared-elevator configuration by using two analytical methods based on subsonic lifting-surface theory. Both methods analyzed the stabilizer and elevator as a single, deforming surface, but one method also allowed the elevator to be analyzed as hinged from the stabilizer. All analyses predicted lower flutter dynamic pressures than experiment with best agreement (within 12 percent) for the hinged-elevator method. Considering the model as mounted from a flexible rather than rigid sting in the analyses had only a slight effect on the flutter results but was significant in that a sting-related vibration mode was identified as a potentially flutter-critical mode.

17. Key Words (Suggested by Author(s))	18. Distribution Statement
Flutter Geared elevator Transonic effects Aeroelasticity	Unclassified - Unlimited Subject Category 05

19. Security Classif. (of this report)	20. Security Classif. (of this page)	21. No. of Pages	22. Price*
Unclassified	Unclassified	27	$4.50

For sale by the National Technical Information Service, Springfield, Virginia 22161

NASA-Langley, 1980